# Appendix for Ikeuchi et al.

## Table of Contents

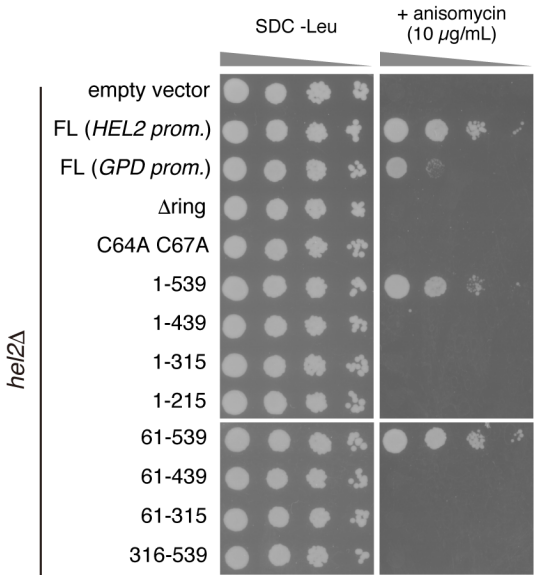


**Appendix Figure S1.** The anisomycin sensitivity of the Hel2 mutants.

Spot assay of the Hel2 mutants with or without anisomycin. Yeast *hel2*Δ cells harboring plasmids expressing N-terminally HA-tagged Hel2 mutant series (used in Main Figure 1 B-D) were cultured in liquid SDC -Leu media at 30ºC for 1 day. The cells were diluted to OD600 = 0.3 as basal spots, and 10-fold serial dilutions were prepared. The serial dilutions were grown on SDC -Leu media with or without 10 μg/mL of anisomycin at 30ºC for 2 days.

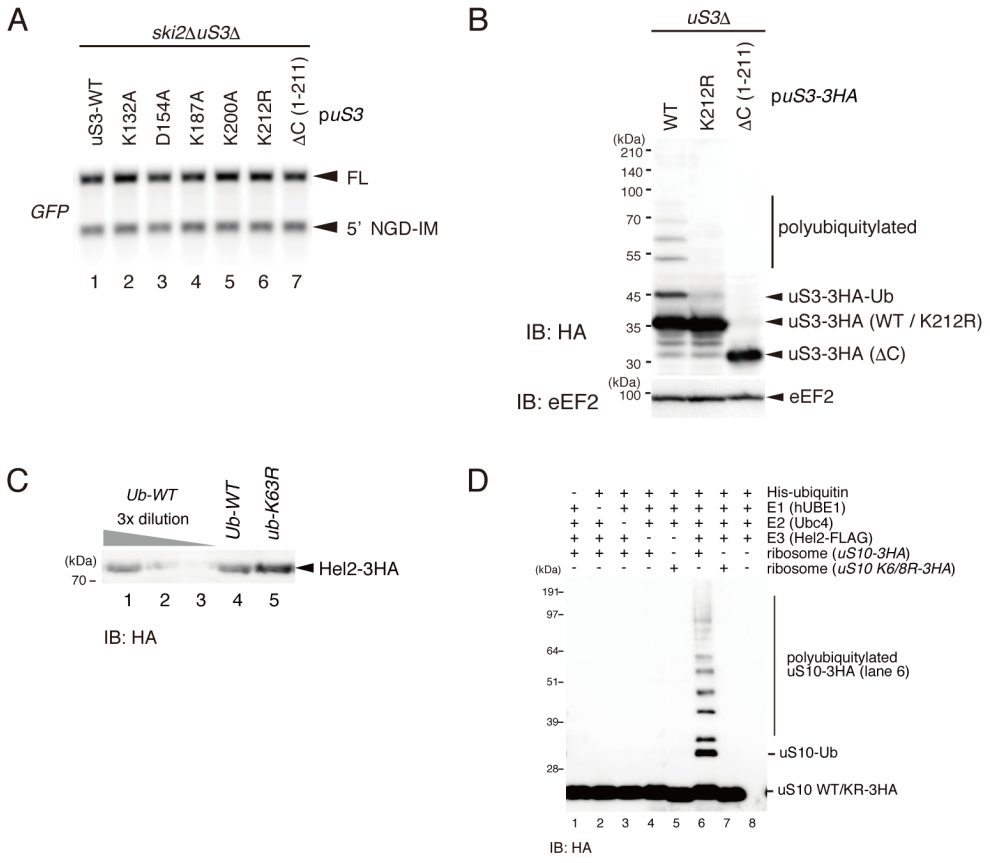


**Appendix Figure S2.** Ubiquitination of uS3 at K212 is does not is not necessary to induce endonucleolytic cleavage caused by the $R(CGN)_{12}$ sequence.

**(A)** The *GFP-R(CGN)$_{12}$-HIS3* mRNA (FL) and 5' NGD-intermediate (5'NGD-IM) were detected by Northern blot analysis in the *ski2*Δ*uS3*Δ strains expressing the indicated plasmid-derived uS3 mutant proteins with the DIG-labelled *GFP* probe. *SCR1* was used as a loading control. ΔC is a uS3 mutant lacking C-terminal tail (212-240 residues). **(B)** Western blot analysis showing that lysine(K)212 of uS3 is a solely responsible for the uS3 ubiquitination. The ubiquitinated forms of uS3 in the indicated strains expressing wild type or mutant uS3-3HA were detected using an anti-HA antibody. **(C)** Western blot analysis showing that the expression level of Hel2 was not decreased in a strain expressing a K63R mutant (ub-K63R) of ubiquitin. **(D)** Western blot analysis of *in vitro* ubiquitination assay with the indicated purified proteins and ribosomes containing HA-tagged uS10 or the indicated uS10 mutants showing Hel2-mediated polyubiquitination of uS10 at K6 and K8 residues. Poly-ubiquitinated uS10-3HA was detected with anti-HA antibody.

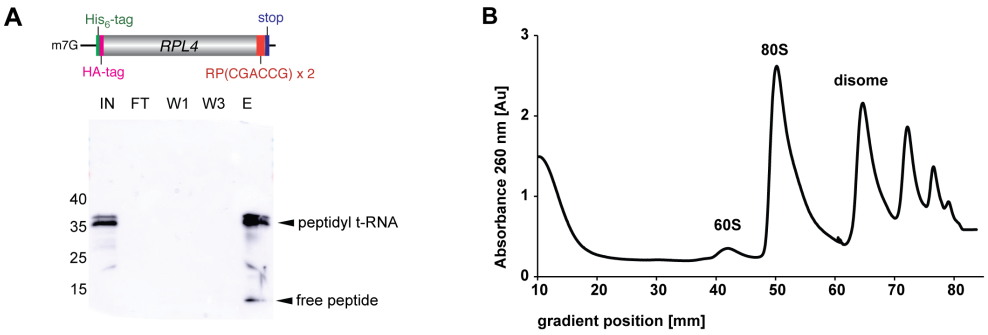


**Appendix Figure S3.** Characterization of the CGA-CCG reporter mRNA and purification of the (CGA-CCG)-dicodon stalled RNCs.

**(A)** Top: Schematic drawing of *His-HA-uL4-(CGA-CCG)*$_2$ reporter. Bottom: *His-HA-uL4-(CGA-CCG)*$_2$ mRNA was added to a yeast *in vitro* translation extract obtained from a *ski2*Δ strain. After the translation reaction, the extract was added to Dynabeads™ (Invitrogen) for affinity purification of His-tagged ribosome nascent chain complexes. The beads were washed three times and eluted using imidazole. 1/100 of each sample was taken for Western blot analysis using an anti-HA antibody. **(B)** The eluate was loaded on a 10-50 % sucrose gradient and fractionated. Peaks for 80S monosomes and disomes were collected and ribosomes were pelleted through a sucrose cushion. Resuspended pellets were used for cryo-EM.

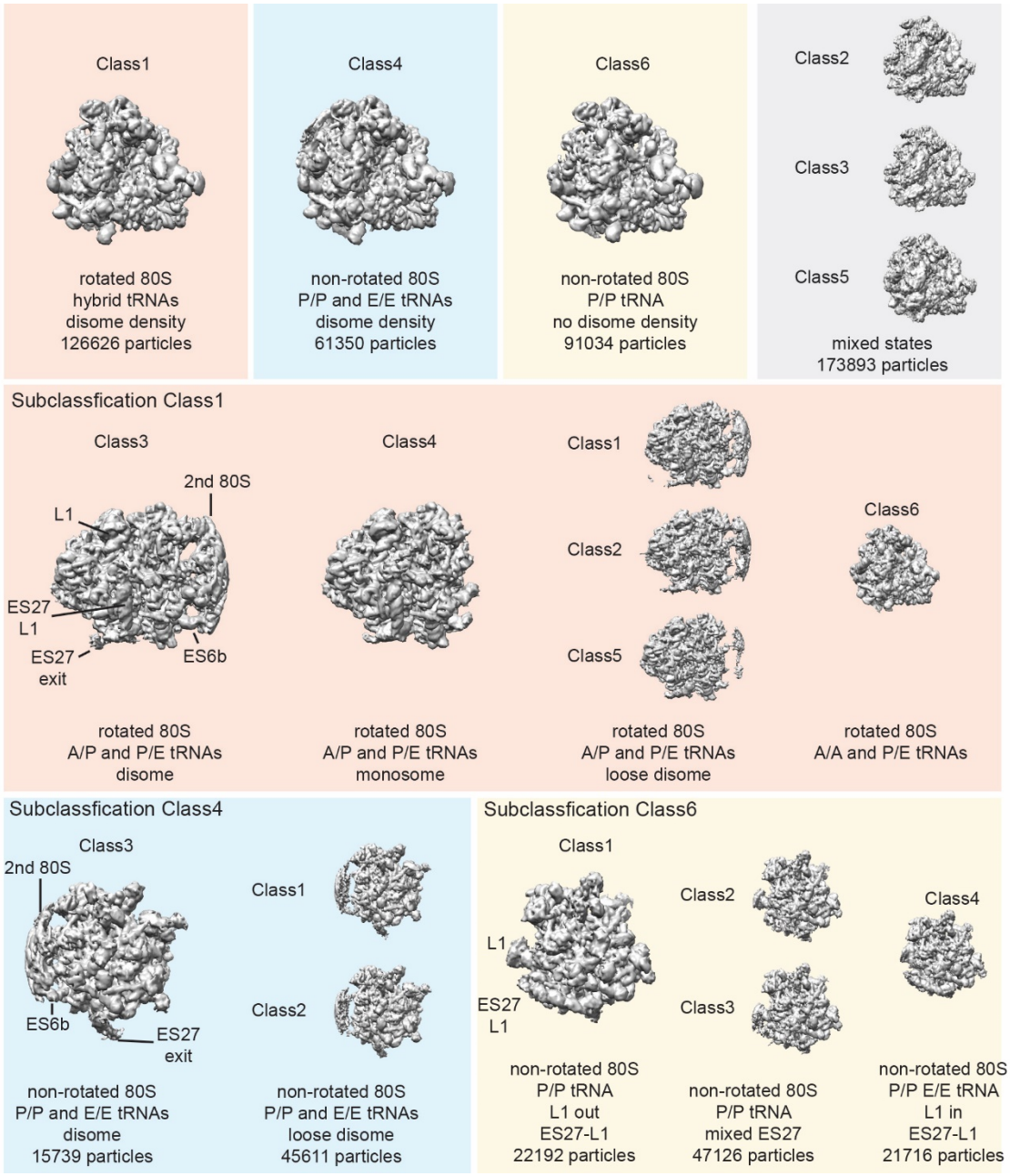


**Appendix Figure S4.** 3D classification scheme for the disome reconstruction (first part).

The disome dataset was initially processed like 80S monosomes (see methods). The first refined map was 3D classified into 6 classes. Class1 showed rotated state ribosomes with hybrid tRNAs and class4 showed a programmed ribosome in the non-rotated POST state occupied with P/P and E/E site tRNAs. Class 6 contained mainly P-site tRNA and rRNA expansion segment ES27 in a position facing the L1-stalk (L1 position). In class 1 and 4 extra density was observed either close to the mRNA exit site (class 4) or the mRNA entry site (class 1) whereas class 6 contained no

extra densities at the mRNA entry and exit sites. Classes 2, 3 and 5 were either low populated or noisy and were not further processed. Classes 1, 4 and 6 were further sub-classified (red, blue and yellow fields). Class 1 was sub-sorted into 6 classes, one of which (class 3) showed a defined extra density for a second ribosome. Class 4 was sub-sorted into 3 classes, one of which (class 3) showed a defined extra density for a second ribosome, hybrid A/P and P/E tRNAs and rearranged ES6c. Another class (class 4) showed a rotated monosome (not involved in disome formation). Class 6 from the first classification was sub-sorted into 4 classes, of which one class (class 1) showed ES27 in the L1 position. All maps displayed in big size were further refined (Appendix Fig S6).

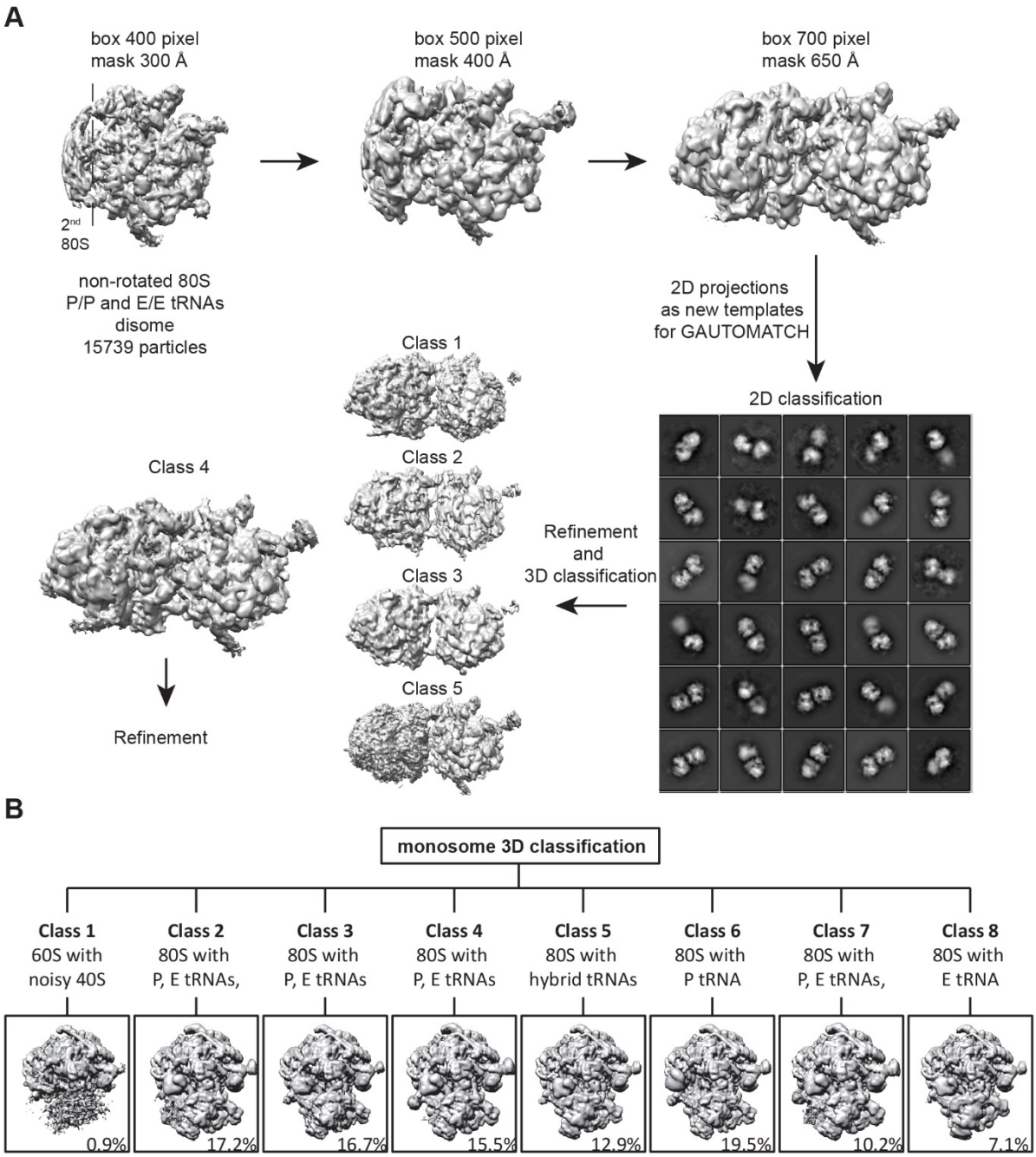


**Appendix Figure S5.** Reconstruction of the disome and 3D classification of the CGA-CCG stalled monosome dataset.

**(A)** The 3D reconstruction of the P/P and E/E tRNAs containing ribosome contained extra density for a second ribosome. To obtain the disome, the respective particles were re-extracted and refined using larger box sizes and mask diameters, revealing first features of a 40S subunit adjacent to the mRNA exit and, after a second re-extraction entire disome. Notably the second ribosome

showed up in the rotated state with A/P and P/E tRNAs. The disome map was used as a new template for particle picking in GAUTOMATCH. Particles were extracted and rescaled for 2D classification. This yielded in several classes clearly showing the shape of a stably formed disome and 107872 particles were selected, initially refined and 3D classified into 5 classes. One class (class 4) showed a defined arrangement of the disome, whereas the other four classes showed less clear features in the interface (class 2 and 3) and/or one ribosome poorly resolved (class 1 and 5) and particles representing stable disomes (27719 particles) were further refined. **(B)** A small dataset was collected for the CGA-CCG stalled monosome (the leading ribosome only) resulting in approx. 100000 particles after 2D classification. The particles were classified into 8 classes, of which four (86,2 %) contained tRNAs in the P/P and E/E sites (empty A site) and only one class with tRNAs in the hybrid sites. Thus, the majority of particles is in the conformation of the leading ribosome of disome.

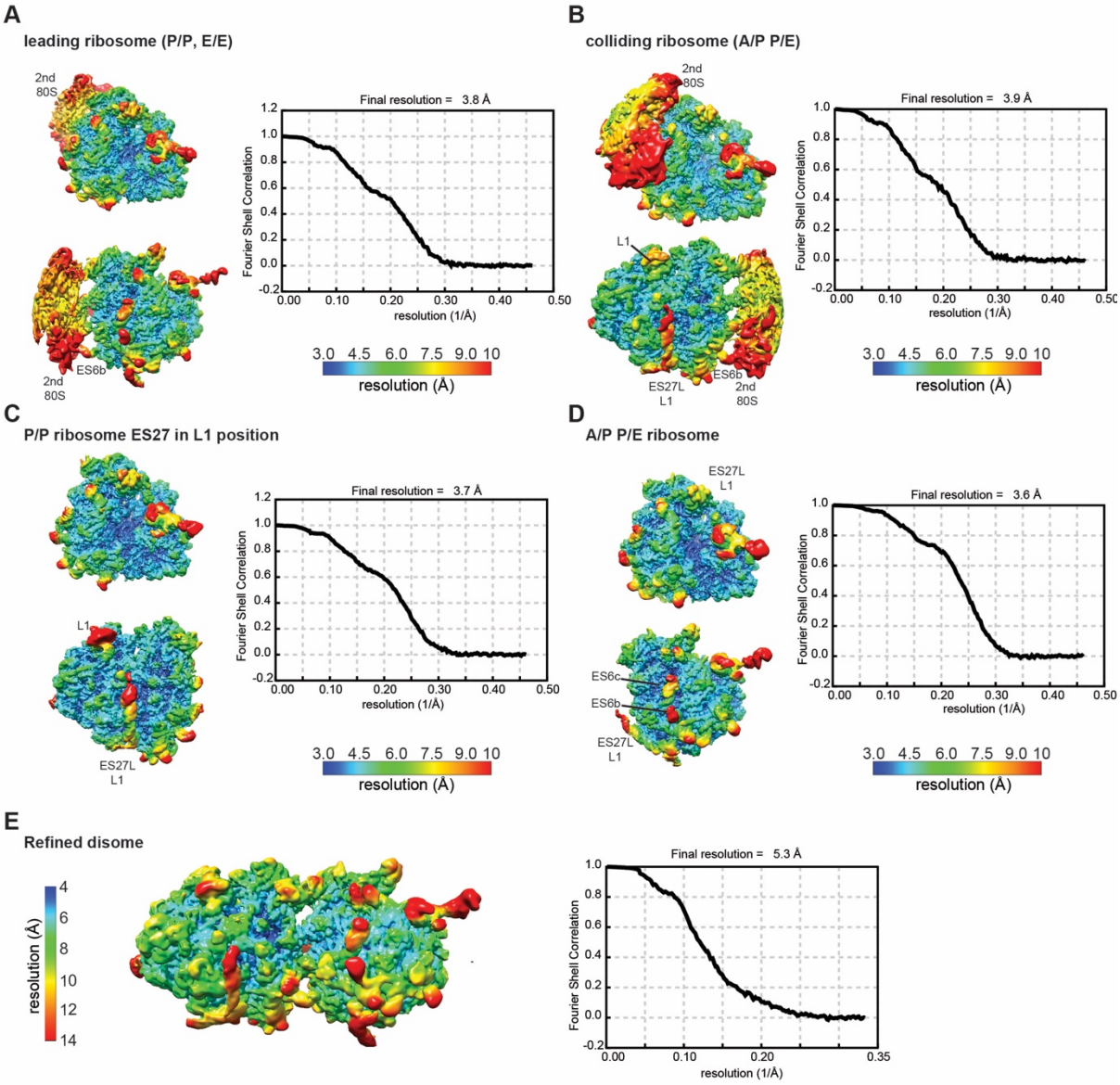


**Appendix Figure S6.** Local resolution and FSC curves for the disome and sub-sorted monosome populations.

Resolution and local resolution was calculated in RELION-2.0. 3D maps are colored according to local resolution and FSC curves are shown for the individually refined leading **(A)** and colliding **(B)** ribosomes as well as for two monosomes not involved in disome formation. One is in the same state as the leading ribosome (POST state with P/P tRNA; **(C)**) and one in the same state as the colliding ribosome (rotated state with A/P and P/E tRNAs; **(D)**). Ribosomes differ in conformations of ES27L and ES6c. The overall resolution for monosome reconstructions ranged

from 3.6 to 3.9 Å according to the “gold standard” criterion and the overall resolution of the disome. **(E)** was 5.3 Å with local resolution ranging from below 4 Å in the ribosomal cores until above 10 Å for flexible elements. In the interface, local resolution was between 5 and 10 Å allowing to rigid-body fit molecular models for the ribosomal RNA and proteins.

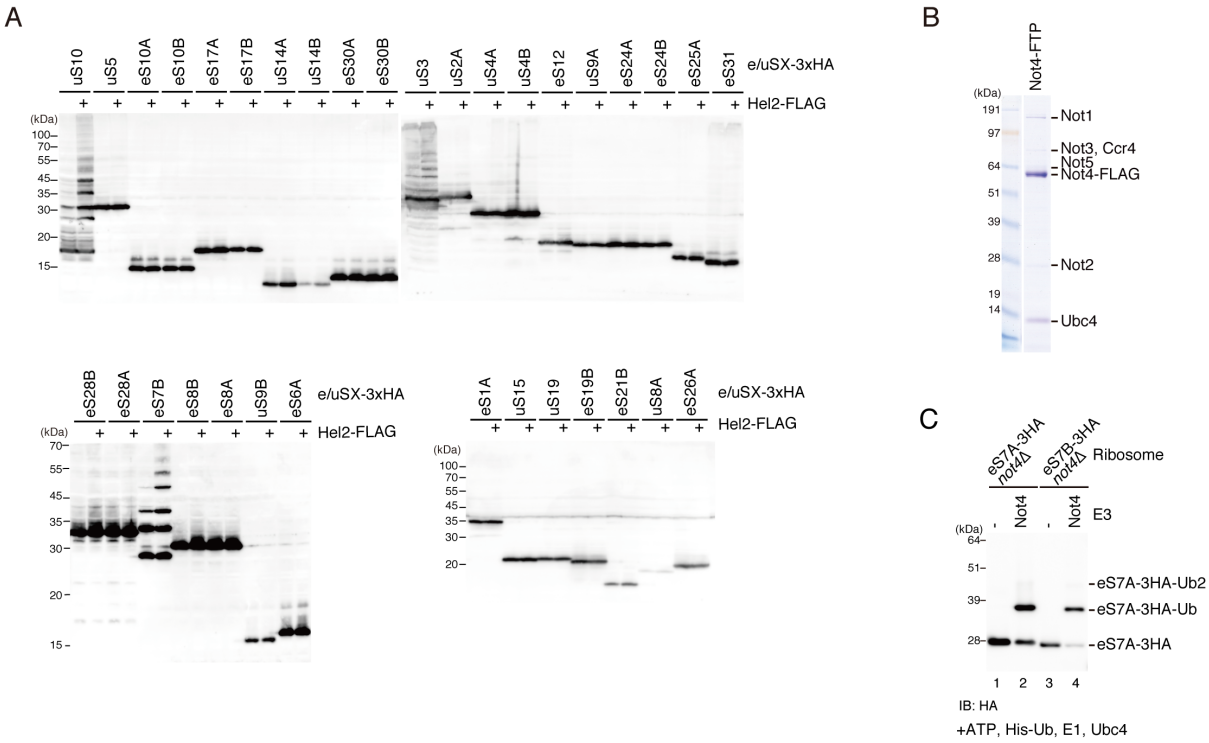


**Appendix Figure S7.** Hel2 ubiquitinates eS7A in a Not4-dependent manner.

**(A)** Western blot analysis showing that overexpression of Hel2 increased the polyubiquitinated form of ribosomal proteins eS7, uS10 and uS3. All indicated ribosomal proteins were HA-tagged and the levels of (poly)-ubiquitinated ribosomal-proteins were detected using an anti-HA antibody **(B)** SDS-PAGE and CBB-staining after affinity purification of tagged Not4 showing that additional components of the Ccr4-NOT complex are co-purified. This preparation was used in *in vitro* ubiquitination assays. **(C)** Western blotting of an *in vitro* ubiquitination assay showing that Not4 is required and sufficient for mono-ubiquitination of both eS7A and eS7B. The reaction was performed using the indicated purified proteins and ribosomes containing HA-tagged eS7A or eS7B.

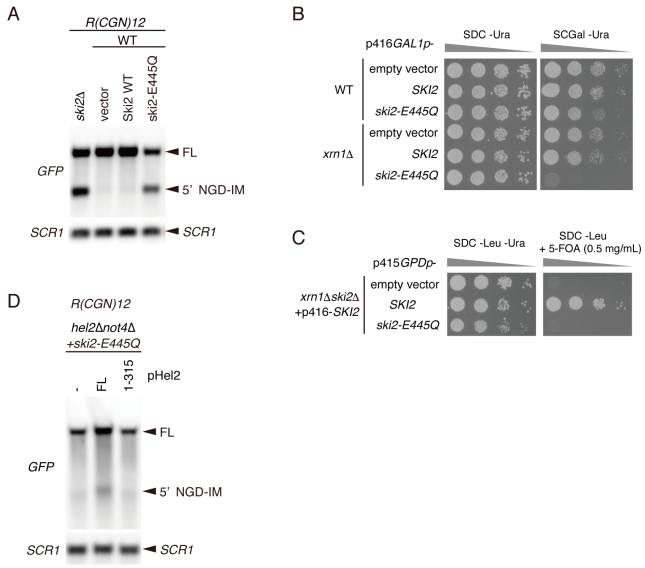


**Appendix Figure S8.** Ski2-E445Q mutant exhibits dominant negative effect in exosome-mediated 3' to 5' mRNA decay.

(A) Northern blot analysis showing that overexpression of ski2-E445Q in wild-type cells inhibited the exosome-mediated decay of 5'NGD intermediates. 5'NGD intermediates (5'NGD-IM) are detectable in *ski2*Δ cells and wild-type cells with ski2-E445Q overexpression, but not in wild-type cells harboring empty vector nor with Ski2 wild-type overexpression. **(B)** Spot assay showing that ski2-E445Q overexpression caused synthetic sick of *xrn1*Δ cells. Yeast wild-type and *xrn1*Δ cells harboring empty vector or plasmids expressing Ski2 wild-type or E445Q mutant by *GAL1* promoter, were cultured in liquid SC 2% Raffinose -Ura media at 30ºC for 1 day. The cells were diluted to OD600 = 0.3 as basal spots, and 10-fold serial dilutions were prepared. The serial dilutions were grown on SDC -Ura or SC 2% galactose -Ura media at 30ºC for 2 days. **(C)** Spot assay showing that ski2-E445Q expression did not rescue *xrn1*Δ*ski2*Δ cells. Yeast *xrn1*Δ*ski2*Δ cells harboring p416*GPDp-SKI2* were transformed with p415*GPD* empty vector, p415*GPDp-SKI2* wild-type or *E445Q*, were cultured in liquid SDC -Leu media at 30ºC for 1 day. The cells were diluted to OD600 = 0.3 as basal spots, and 10-fold serial dilutions were prepared. The serial dilutions were grown on SDC -Leu -Ura or SDC -Leu with 0.5 mg/ml 5-fluoroorotic acid (5-FOA) media at 30ºC for 2 days. **(D)** Northern blot analysis showing that Hel2 1-315 mutant expression failed to induce mRNA cleavages in *hel2*Δ*not4*Δ mutant cells. 5'NGD intermediates (5'NGD-IM) are detected in ski2-E445Q overexpression condition.

**Appendix Table S1**

**Yeast strains used in study**

| Strains name | Genotype/plasmid | Source |
|---|---|---|
| W303-1a | *MAT*a *ade2 his3 leu2 trp1 ura3 can1* | Lab. Stock, Parent |
| YIT2002 | *not4*Δ*::kanMX4* | Dimitrova *et al.* 2009 |
| YIT2004 | *upf1*Δ*::kanMX4* | Kuroha *et al.* 2009 |
| YIT2011 | *asc1*Δ*::kanMX4* | Kuroha *et al.* 2010 |
| YIT2025 | *ltn1*Δ*::kanMX4* | Matsuda *et al*. 2014 |
| YKI110 | *hel2*Δ*::natMX4* | Matsuo *et al*. 2017 |
| YKI339 | *ubc4*Δ*::natMX4* | Matsuo *et al*. 2017 |
| YKI567 | *hel2*Δ*::natMX4 ltn1*Δ*::kanMX4* | Matsuda *et al*. 2014 |
| YKI1720 | *slh1*Δ*::natMX4* | Matsuo *et al*. 2017 |
| YKI1887 | *rqc2*Δ*::hphMX4* | Matsuo *et al*. 2017 |
| YKS196 | *hel2*Δ*::natMX4, not4*Δ*::HIS3MX6* | This study |
| YKS224 | *slh1*Δ*::natMX4, not4*Δ*::HIS3MX6* | This study |
| YIT2013 | *ski2*Δ*::kanMX4* | Kuroha *et al.* 2010 |
| YKI112 | *ski2*Δ*::kanMX4, hel2*Δ*::natMX4* | This study |
| YKK924 | *ski2*Δ*::natMX4, not4*Δ*::kanMX4* | This study |
| YKI102 | *ski2*Δ*::kanMX4, ubc4*Δ*::natMX4* | This study |
| YKI315 | *ski2*Δ*::kanMX4, ubc5*Δ*::hphMX4* | This study |
| YKI1726 | *ski2*Δ*::kanMX4, slh1*Δ*::natMX4* | This study |
| YKI2012 | *ski2*Δ*::kanMX4, slh1*Δ*::natMX4, not4*Δ*::hphMX4* | This study |
| YKI972 | *ski2*Δ*::kanMX4, uS10*Δ*::natMX4, p416GPDp-uS10-CYC1t* | This study |
| YKI970 | *ski2*Δ*::kanMX4, uS3*Δ*::natMX4, p416GPDp-uS3-CYC1t* | This study |
| YKI1087 | *ski2*Δ*::kanMX4, uS3*Δ*::natMX4, uS10*Δ*::hphMX4, p414GPDp-uS3-K212R-CYC1t, p416GPDp-uS10-CYC1t* | This study |
| YKI2025 | *ski2*Δ*::kanMX4, uS10*Δ*::natMX4, not4*Δ*::hphMX4, p416GPDp-uS10-CYCt* | This study |

| | | |
|---|---|---|
| YKI2002 | *ski2*Δ*::kanMX4, eS7A*Δ*::HIS3MX6, eS7B*Δ*::natNT2, p416-eS7Ap-eS7A* | This study |
| YKI2006 | *ski2*Δ*::hphMX4, slh1*Δ*::kanMX4, eS7A*Δ*::HIS3MX6, eS7B*Δ*::natNT2, p416-eS7Ap-eS7A* | This study |
| YIT2019 | *xrn1*Δ*::kanMX4* | Tsuboi *et al*. 2012 |
| YKI522 | *xrn1*Δ*::kanMX4, hel2*Δ*::natMX4* | This study |
| YKI523 | *xrn1*Δ*::kanMX4, ubc4*Δ*::natMX4* | This study |
| YKI105 | *xrn1*Δ*::kanMX4, asc1*Δ*::natMX4* | This study |
| YAI575 | *xrn1*Δ*::kanMX4, slh1*Δ*::natMX4* | This study |
| YKI1456 | *xrn1*Δ*::kanMX4, uS10*Δ*::natMX4, p416GPDp-uS10-CYC1t* | This study |
| YKI2024 | *xrn1*Δ*::kanMX4, not4*Δ*::natMX4, p416GPDp-FLAG-NOT4-CYC1t* | This study |
| YKI2026 | *xrn1*Δ*::kanMX4, ski2*Δ*::natMX4, p416GPDp-SKI2-CYC1t* | This study |
| YKI1183 | *hel2*Δ*::kanMX4, uS10*Δ*::natMX4, p416GPDp-uS10-CYC1t* | Matsuo *et al*. 2017 |
| YKI1747 | *HEL2-FTP::natNT2, uS10*Δ*::kanMX4, p416GPDp-uS10-CYC1t* | Matsuo *et al*. 2017 |
| YYS2191 (*UB-WT*) | *MATa lys2-801 leu2-3,2-112 ura3-52 his3-*Δ*200 trp1-1 ubi1-*Δ*1::TRP1 ubi2-*Δ*2::ura3 ubi3-*Δ*ub-2 ubi4-*Δ*2::LEU2 (YEpKan-TEF1p-kozak-yUb-CYC1t) (pUB100)* | This study, parental strain is SUB328 (DF5, Finley Lab.) |
| YYS2192 (*ub-K63R*) | *MATa lys2-801 leu2-3,2-112 ura3-52 his3-*Δ*200 trp1-1 ubi1-*Δ*1::TRP1 ubi2-*Δ*2::ura3 ubi3-*Δ*ub-2 ubi4-*Δ*2::LEU2 (YepKan-TEF1p-kozak-yUbK63R-CYC1t) (pUB100)* | This study, parental strain is SUB328 (DF5, Finley Lab.) |
| YKI1660 | YYS2191*, ski2*Δ*::natMX4* | This study |
| YKI1663 | YYS2192*, ski2*Δ*::natMX4* | This study |
| YKI1969 | YYS2191*, uS10-3HA::natNT2* | This study |
| YKI1970 | YYS2192*, uS10-3HA::natNT2* | This study |
| YKI1662 | YYS2191*, ltn1*Δ*::natMX4* | This study |

| | | |
|---|---|---|
| YKI1665 | YYS2192, *ltn1Δ::natMX4* | This study |
| Y124 | *eS7AΔ::HIS3MX6, eS7BΔ::natNT2, p416-eS7Ap-eS7A* | This study |
| YYM237 | *hel2Δ::kanMX4, eS7AΔ::HIS3MX6, eS7BΔ::natNT2, p416-eS7Ap-eS7A* | This study |
| YKS1327 | *slh1Δ::kanMX4, eS7AΔ::HIS3MX6, eS7BΔ::natNT2, p416-eS7Ap-eS7A* | This study |
| YKS193 | *not4Δ::kanMX4, eS7AΔ::HIS3MX6, eS7BΔ::natNT2, p416-eS7Ap-eS7A* | This study |
| Y46 | *uS10(RPS20)-3HA::HIS3MX6* | This study |
| Y47 | *uS3(RPS3)-3HA::HIS3MX6* | This study |
| Y48 | *eS7A(RPS7A)-3HA::HIS3MX6* | This study |
| Y49 | *eS7B(RPS7B)-3HA::HIS3MX6* | This study |
| Y85 | *not4Δ::kanMX4, eS7A-3HA::HIS3MX6* | This study |
| Y86 | *not4Δ::kanMX4, eS7B-3HA::HIS3MX6* | This study |
| Y87 | *hel2Δ::natMX4, uS10-3HA::HIS3MX6* | This study |
| Y89 | *hel2Δ::natMX4, eS7A-3HA::HIS3MX6* | This study |
| Y90 | *hel2Δ::natMX4, eS7B-3HA::HIS3MX6* | This study |
| YSG0 | *RPS0A-3HA::HIS3MX6* | This study |
| YSG2 | *RPS1A-3HA::HIS3MX6* | This study |
| YSG34 | *RPS2-3HA::HIS3MX6* | This study |
| YSG6 | *RPS6A-3HA::HIS3MX6* | This study |
| YSG10 | *RPS8A-3HA::HIS3MX6* | This study |
| YSG11 | *RPS8B-3HA::HIS3MX6* | This study |
| YSG41 | *RPS9A-3HA::HIS3MX6* | This study |
| YSG44 | *RPS9B-3HA::HIS3MX6* | This study |
| YSG12 | *RPS10A-3HA::HIS3MX6* | This study |
| YSG13 | *RPS10B-3HA::HIS3MX6* | This study |
| YSG14 | *RPS12-3HA::HIS3MX6* | This study |
| RPS13-3HA | *RPS13-3HA::HIS3MX6* | This study |
| YSG54 | *RPS15-3HA::HIS3MX6* | This study |
| RPS16A-3HA | *RPS16A-3HA::HIS3MX6* | This study |
| RPS16B-3HA | *RPS16B-3HA::HIS3MX6* | This study |

| | | |
|---|---|---|
| YSG15 | *RPS17A-3HA::HIS3MX6* | This study |
| YSG16 | *RPS17B-3HA::HIS3MX6* | This study |
| YSG18 | *RPS19B-3HA::HIS3MX6* | This study |
| YSG20 | *RPS21B-3HA::HIS3MX6* | This study |
| RPS22A-3HA | *RPS22A-3HA::HIS3MX6* | This study |
| YSG21 | *RPS24A-3HA::HIS3MX6* | This study |
| YSG22 | *RPS24B-3HA::HIS3MX6* | This study |
| YSG23 | *RPS25A-3HA::HIS3MX6* | This study |
| YSG25 | *RPS26A-3HA::HIS3MX6* | This study |
| YSG29 | *RPS28A-3HA::HIS3MX6* | This study |
| RPS28B-3HA | *RPS28B-3HA::HIS3MX6* | This study |
| RPS29A-3HA | *RPS29A-3HA::HIS3MX6* | This study |
| RPS29B-3HA | *RPS29B-3HA::HIS3MX6* | This study |
| YSG31 | *RPS30A-3HA::HIS3MX6* | This study |
| YSG32 | *RPS30B-3HA::HIS3MX6* | This study |
| YSG33 | *RPS31-3HA::HIS3MX6* | This study |

**Appendix Table S2**

**Plasmids used in study**

| Plasmid name | Feature | Source |
|---|---|---|
| p416*GPDp* | *CEN6, URA3, GPD promoter* | Mumberg *et al.* 1995 |
| p415*GPDp* | *CEN6, LEU2, GPD promoter* | Mumberg *et al.* 1995 |
| p414*GPDp* | *CEN6, TRP1, GPD promoter* | Mumberg *et al.* 1995 |
| p416*GAL1p* | *CEN6, URA3, GAL1 promoter* | Mumberg *et al.* 1994 |
| pRS315 | *CEN6, LEU2* | Mumberg *et al.* 1995 |
| | | |
| pSA144 | p416*GPDp-GFP-FLAG-HIS3-CYC1t* | Dimitrova *et al.* 2009 |
| pIT827 | yCplac33*GAL1p-FLAG-his3-ns* | Inada and Aiba, 2005 |
| pIT2004 | p416*GPDp-GFP-R(CGN)12-FLAG-HIS3-CYC1t* | Dimitrova *et al.* 2009 |
| pIT2024 | p416*GPDp-GFP-G-quadruplex-FLAG-HIS3-CYC1t* | Dimitrova *et al.* 2009 |
| pIT2043 | p416*GAL1p-FLAG-his3-100 (UAA at 100th codon) - CYC1t* | Kuroha et al. 2009 |
| pIT2051 | p416*GPDp-GFP-K(AAA)12-FLAG-HIS3-CYC1t* | Dimitrova *et al.* 2009 |
| pIT2101 | p416*GPDp-GFP-Rare-FLAG-HIS3-CYC1t* | Tsuboi *et al.* 2012 |
| pIT2104 | p416*GAL1p-GFP-FLAG-HIS3-CYC1t* | Tsuboi *et al.* 2012 |
| pIT2105 | p416*GAL1p-GFP-Rz-FLAG-HIS3-CYC1t* | Tsuboi *et al.* 2012 |
| pIT2123 | p416*GAL1p-GFP-K(AAA)12-FLAG-HIS3-CYC1t* | Tsuboi *et al.* 2012 |
| pLD38 | p416*GAL1p-GFP-R(CGN)12-FLAG-HIS3-CYC1t* | This study |
| pKK61 | p414*GPDp-GFP-R(CGN)12-FLAG-HIS3-CYC1t* | This study |
| pKI74 | p415*GPDp-SKI2-CYC1t* | Ikeuchi and Inada, 2016 |
| pKI75 | p415*GPDp-ski2-E445Q-CYC1t* | Ikeuchi and Inada, 2016 |
| pKI347 | p416*GPDp-SKI2-CYC1t* | This study |
| pKI355 | p416*GAL1p-SKI2-CYC1t* | This study |
| pKI356 | p416*GAL1p-ski2-E445Q-CYC1t* | This study |
| pKI19 | p415*GPDp-HEL2-FLAG-CYC1t* | Matsuo *et al*. 2017 |
| pKI31 | p415*GPDp-hel2* Δ*ring-FLAG-CYC1t* | Matsuo *et al*. 2017 |
| pKI32 | p415*GPDp- hel2-C64/67A-FLAG-CYC1t* | Matsuo *et al*. 2017 |

| | | |
|---|---|---|
| pDS14 | p415*GPDp- hel2 (1-315 a.a.)-FLAG-CYC1t* | This study |
| pKI89 | p415*GPDp-HA-HEL2-CYC1t* | This study |
| pKI90 | p415*GPDp-HA- hel2-Δring-CYC1t* | This study |
| pKI91 | p415*GPDp-HA- hel2-C64A/C67A-CYC1t* | This study |
| pKI92 | p415*GPDp-HA- hel2 (1-539 a.a.)-CYC1t* | This study |
| pKI93 | p415*GPDp-HA- hel2 (1-439 a.a.)-CYC1t* | This study |
| pKI94 | p415*GPDp-HA- hel2 (1-315 a.a.)-CYC1t* | This study |
| pKI95 | p415*GPDp-HA- hel2 (1-215 a.a.)-CYC1t* | This study |
| pKI99 | p415*GPDp-HA- hel2 (61-539 a.a.)-CYC1t* | This study |
| pKI100 | p415*GPDp-HA- hel2 (61-439 a.a.)-CYC1t* | This study |
| pKI101 | p415*GPDp-HA- hel2 (61-315 a.a.)-CYC1t* | This study |
| pKI102 | p415*GPDp-HA- hel2 (316-539 a.a.)-CYC1t* | This study |
| pKI106 | p415*HEL2p-HEL2-FLAG-CYC1t* | This study |
| pKI45 | p416*GPDp-uS10(RPS20)-CYC1t* | Matsuo *et al*. 2017 |
| pKI80 | p415*GPDp-uS10-CYC1t* | Matsuo *et al*. 2017 |
| pKI81 | p415*GPDp-uS10-K6/8R-CYC1t* | Matsuo *et al*. 2017 |
| pKI124 | p414-*uS10p-uS10-CYC1t* | This study |
| pKI140 | p414-*uS10p-uS10-K6/8R-CYC1t* | This study |
| pKI236 | p414-*uS10p-uS10-3HA-CYC1t* | This study |
| pKI237 | p414-*uS10p-uS10-K6/8R-3HA-CYC1t* | This study |
| pKI44 | p416*GPDp-uS3(RPS3)-CYC1t* | Matsuo *et al*. 2017 |
| pKI46 | p414*GPDp-uS3-CYC1t* | Matsuo *et al*. 2017 |
| pKI49 | p414*GPDp-uS3-K132A-CYC1t* | This study |
| pKI50 | p414*GPDp-uS3-D154A-CYC1t* | This study |
| pKI51 | p414*GPDp-uS3-K187A-CYC1t* | This study |
| pKI52 | p414*GPDp-uS3-K200A-CYC1t* | This study |
| pKI53 | p414*GPDp-uS3-K212R-CYC1t* | Matsuo *et al*. 2017 |
| pKI54 | p414*GPDp-uS3-ΔC (1-211 a.a.)-CYC1t* | This study |
| pKI269 | p414-*uS3p-uS3-3HA-CYC1t* | This study |
| pKI270 | p414*GPDp-uS3p-uS3-K212R-3HA-CYC1t* | This study |
| pKI271 | p414*GPDp-uS3-ΔC (1-211 a.a.)-3HA-CYC1t* | This study |
| pKI260 | p416*HEL2p-ProteinA-TEV-His6-HEL2-CYCt* | This study |

| | | |
|---|---|---|
| pFS3 | p415*GPDp-uL23(RPL25)-FLAG-CYC1t* | Matsuo *et al*. 2017 |
| pIT2172 | p415*GPDp-uS5(RPS2)-FLAG-CYC1t* | Ikeuchi and Inada, 2016 |
| pKI312 | p416*GPDp-NOT4-FLAG-TEV-ProteinA-ADH1t* | This study |
| pRM13 | p415*GPDp-FLAG-NOT4-CYC1t* | This study |
| pKI346 | p416*GPDp-FLAG-NOT4-CYC1t* | This study |
| p315-7A | pRS315-*eS7Ap-eS7A(RPS7A)-HA* | This study |
| p315-4KR | pRS315-*eS7Ap-eS7A-4KR(K72/76/83/84R)-HA* | This study |
| pSG201 | pRS315-*eS7Ap-eS7A-K72single(K76/83/84R)-HA* | This study |
| pSG202 | pRS315-*eS7Ap-eS7A-K76single(K72/83/84R)-HA* | This study |
| pSG203 | pRS315-*eS7Ap-eS7A-K83single(K72/76/84R)-HA* | This study |
| pSG204 | pRS315-*eS7Ap-eS7A-K84single(K72/76/83R)-HA* | This study |
| pGEX-UBC4 | pGEX-*UBC4 (ampR, for recombinant protein expression in E. coli)* | This study |